

Cite this: *RSC Adv.*, 2014, 4, 54960

## Aqueous-phase catalytic oxidation of furfural with H<sub>2</sub>O<sub>2</sub>: high yield of maleic acid by using titanium silicalite-1†

N. Alonso-Fagúndez,<sup>a</sup> I. Agirrezabal-Telleria,<sup>b</sup> P. L. Arias,<sup>b</sup> J. L. G. Fierro,<sup>a</sup> R. Mariscal<sup>a</sup> and M. López Granados<sup>\*a</sup>

This investigation explores the selective liquid-phase oxidation of furfural to maleic acid (MA) using hydrogen peroxide as an oxidant and titanium silicalite (TS-1) as a catalyst. The effect of temperature and of the concentration of H<sub>2</sub>O<sub>2</sub>, furfural and catalyst on the MA yield was studied. The highest yield, 78 mol%, was obtained under the following reaction conditions: 4.6 wt% of furfural, 4.6 wt% of catalyst, a H<sub>2</sub>O<sub>2</sub>/furfural mol ratio of 7.5, corresponding to 12.3 wt% of H<sub>2</sub>O<sub>2</sub>, 323 K and 24 hours of reaction. To reduce the amount of H<sub>2</sub>O<sub>2</sub> employed, a two-step sequence of reactions was conducted using TS-1 and Amberlyst 70 consecutively as catalysts in the first and second steps, respectively. In this case, a H<sub>2</sub>O<sub>2</sub>/furfural mol ratio = 4.4 was required, which is quite close to the stoichiometric ratio (3.0), and a maleic acid yield close to 80% was obtained under 4.6 wt% of furfural, 4.6 wt% of catalyst and 28 h of reaction at 323 K; after 52 h of reaction, the MA yield reached 92%. Fresh and used catalysts were characterised by X-ray diffraction (XRD), Raman spectroscopy, total reflection X-ray fluorescence (TXRF), X-ray photoelectron spectroscopy (XPS), N<sub>2</sub> adsorption–desorption isotherms and thermogravimetric analysis. Ti was largely incorporated within the silicalite framework, but the presence of some TiO<sub>2</sub> anatase was also confirmed. Ti leaching was observed, especially during the first run but became much less important in successive cycles. Leaching affects both anatase and Ti species within the silicalite framework. Notwithstanding the leaching, when using pure furfural, TS-1 could be reused for six runs without noticeable deactivation, whereas when using furfural directly derived from biomass, weak but visible deactivation occurred upon reutilisation; this deterioration must be related to the presence of some organic products other than furfural.

Received 31st July 2014  
Accepted 13th October 2014

DOI: 10.1039/c4ra11563e

www.rsc.org/advances

## Introduction

Maleic anhydride (MAN) and its hydrated form, maleic acid (MA), are important C<sub>4</sub> chemical intermediates with applications in multiple fields of the chemical industry. They are important raw materials used in the manufacture of unsaturated polyester resins, vinyl copolymers, tetra- and hexahydrophthalic anhydride (curing agents in epoxy resins), surface coatings, lubricant additives, plasticisers, copolymers, agrochemicals, and pharmaceuticals, as well as in the production of  $\gamma$ -butyrolactone, butanediol and tetrahydrofuran. Succinic acid

and fumaric acid, both of which have multiple additional applications, are also synthesised from MA and/or MAN.<sup>1,2</sup> Currently, maleic anhydride is industrially produced primarily by selective oxidation of *n*-butane (it can also be produced from benzene, but this obsolete route has been almost fully displaced for environmental and economic reasons by butane technology).<sup>3</sup> Both MA and MAN are interconverted into one other by hydration–dehydration processes.<sup>1,2</sup>

Alternative routes based on the oxidation of furfural to MAN and MA, either in gas or liquid phase, have been reported by different research groups. Furfural is a chemical currently obtained from the pentoses contained in lignocellulosic agro-residues; approximately 250–400 ktons of furfural are synthesised annually from this carbohydrate feedstock.<sup>4–6</sup> Therefore, these routes from furfural constitute renewable pathways for the manufacture from biomass of MA, MAN and their derived products. Thus, a renewable route for phthalic anhydride formation by Diels–Alder condensation with furan has very recently been demonstrated.<sup>7</sup>

Gas-phase oxidation of furfural to maleic anhydride is a well-known route, and yields up to 75% can be achieved by using

<sup>a</sup>Group of Sustainable Energy and Chemistry (EQS), Institute of Catalysis and Petrochemistry (ICP-CSIC), C/ Marie Curie 2, Campus de Cantoblanco, 28049 Madrid, Spain

<sup>b</sup>Department of Chemical and Environmental Engineering, Engineering School of The University of The Basque Country (UPV/EHU), Alameda Urquijo s/n, Bilbao 48013, Spain. E-mail: mlgranados@icp.csic.es

† Electronic supplementary information (ESI) available: Additional information on experimental details, catalytic activity, other proposals of mechanism of reaction and characterisation of catalysts by TG analyses, XRD, and N<sub>2</sub> adsorption. See DOI: 10.1039/c4ra11563e

vanadium-oxide-based catalysts; cheap air O<sub>2</sub> is used as an oxidising agent.<sup>8–12</sup> However, dilute furfural streams (below 1% v/v) are required to achieve high MAN selectivity. The reaction is conducted at high temperatures (higher than 523 K), and the vaporisation of furfural is required. Both of these features have a negative impact on the energy balance and consequently the economic viability of this process.

Liquid oxidation with O<sub>2</sub> at milder temperatures has also been explored using homogeneous catalysts like phosphomolybdic acid in a water/tetrachloroethane biphasic system, achieving MA yields not larger than 50%.<sup>13,14</sup> Moreover, although milder temperatures are required (383 K), high O<sub>2</sub> pressure (2 MPa) is needed. The reusability of these catalysts has not been proved, which is crucial to evaluate the feasibility of possible industrial applications.

Another liquid-phase alternative that has recently been investigated is furfural oxidation with hydrogen peroxide. So far, the best results using this strategy have been achieved by using either a soluble acid catalyst like H<sub>2</sub>SO<sub>4</sub> and *p*-toluenesulphonic acid or by using solid sulphonic-based catalysts such as sulphonic resins or poly-(styrene sulphonic acid).<sup>15–19</sup> Oxidation with H<sub>2</sub>O<sub>2</sub> seems attractive for industrial application, first because the reaction proceeds under very mild conditions (low temperatures and atmospheric pressure), and second because aqueous furfural solutions can be processed, which is a key advantage. When pure furfural is produced from lignocellulosic agroresidues, the primary raw product is an aqueous furfural solution that must be further purified by an energy-intensive double distillation. Processing primary raw aqueous furfural solutions would imply that distillation steps are not required, which positively impacts the energy and economic balance of the overall process.

However, the main drawback for oxidation with hydrogen peroxide using acid catalysts is the control of selectivity. A wide distribution of products such as MA, succinic acid (SA), fumaric acid (FumA),  $\beta$ -formylacrylic acid or 2(5*H*)-furanone is obtained. This lack of selectivity is a consequence of the very complex reaction network that starts with the Baeyer–Villiger oxidation of furfural to the corresponding ester.<sup>15,16,19</sup> Large H<sub>2</sub>O<sub>2</sub>/furfural ratios (much larger than 7) are required to improve the MA yield, whereas for lower ratios succinic acid is the main product. Maleic acid could be obtained by dehydrogenation of succinic acid,<sup>20</sup> but this would mean an additional step. The identification of a robust solid catalyst that can selectively oxidise furfural to MA in one step and that can be easily recovered from the reaction mixture and reutilised for a large number of runs is still a challenge.

The selective oxidation of furan with aqueous H<sub>2</sub>O<sub>2</sub> using TS-1 has been already investigated.<sup>21,22</sup> The furan ring possesses a similar chemical structure to furfural, except for the absence of the aldehydic functional group. Maleic dialdehyde and 5-hydroxy-furan-2(5*H*)-one were obtained selectively by the oxidation of furan using H<sub>2</sub>O<sub>2</sub>/furan with approximate mol ratios of 1 and 2, respectively. These products are closely related to maleic acid, as the latter can be obtained from them by further oxidation. Titanium silicalite 1 (TS-1) is frequently used in the epoxidation of numerous alkenes.<sup>23–25</sup> The ability of TS-1

to activate hydrogen peroxide is linked to the particular environment of Ti(IV) cations incorporated into the silicalite framework and located within the hydrophobic pores of the zeolite. This allows simultaneous adsorption of the hydrophobic substrate and the oxidant.<sup>21,26,27</sup>

The latter results using furan encouraged us to explore the utilisation of TS-1 in the selective oxidation of furfural to MA by using H<sub>2</sub>O<sub>2</sub>. Because the oxidation of furfural (a C<sub>5</sub> aldehyde) to maleic acid (a C<sub>4</sub> diacid) implies the loss of a carbon atom, the key question is whether, besides the epoxidation and oxidation steps, the TS-1 catalyst can also promote in practice the removal of a C atom.

In principle the oxidation of furfural with H<sub>2</sub>O<sub>2</sub> is more advantageous than the furan oxidizing route previously demonstrated.<sup>21,22</sup> Furan is currently produced by decarbonylation of furfural<sup>1,2</sup> and therefore the production of MA from furan would imply two steps: first decarbonylation and subsequently the oxidation of furan. A first drawback of this furan route is that the decarbonylation of furfural is conducted at relatively high temperatures (423–453 K) and in the presence of noble metal catalysts that unavoidably deactivate. Reactivation periods are required to regenerate the initial activity that complicates the viability of the furan route. On the contrary the route here proposed implies the direct conversion of furfural in one-step and at mild temperatures.

In this work, we demonstrate for the first time that TS-1 is an excellent catalyst for the transformation of furfural to MA. We have also conducted the necessary study examining the effect of operating variables like temperature, H<sub>2</sub>O<sub>2</sub>/furfural ratio and catalyst and furfural concentration on the catalytic properties of TS-1. Specific attention was paid to the deactivation of catalyst and the reutilisation behaviour of TS-1 under the optimum reaction conditions, using both pure furfural provided by a commercial supplier and aqueous solutions of furfural obtained directly from corncob residues. A commercial TS-1 with a Ti/Si at. ratio above the threshold required to fully saturate the silicalite framework with Ti cations was used in this investigation. This means that a TS-1 with the largest possible incorporation of Ti within silicalite (active sites) was used.

## Experimental

### Materials

Titanium silicalite 1 was purchased from Tricat Zeolites, H-ZSM-5 (Si/Al = 19) was purchased from Akzo Nobel, anatase catalyst support was purchased from Alfa Aesar and Amberlyst-70 was purchased from The Dow Chemical Company. Furfural (99 wt%), hydrogen peroxide (30 wt%), furan (99 wt%) and furan-2(5*H*)-one (98 wt%) were supplied by Sigma-Aldrich. Furoic acid (98 wt%) was provided by Fluka, and oxalic acid (99.5 wt%), used as internal standard, was purchased from Alfa Aesar. 5-Hydroxy-furan-2(5*H*)-one, which was used as a starting reactant, was synthesised according to the findings of Kumar *et al.*,<sup>22</sup> comprising the oxidation of furan with H<sub>2</sub>O<sub>2</sub> using TS-1 as catalyst. Further details of the preparation are given in the ESI section.†

### Catalytic activity measurements

The oxidation of furfural was carried out in a glass flask reactor with three necks: one for the thermocouple, one for the addition of reactants through an addition funnel and the third for sampling through a septum. The required amounts of TS-1 and of H<sub>2</sub>O<sub>2</sub> solution were loaded into the reactor and heated up to the reaction temperature by immersion in an oil bath. After the reaction mixture reached the selected temperature, the reaction started when a known amount of aqueous furfural solution was added to the reactor. To prevent the mixture from cooling down because of the incorporation of the aqueous furfural, the latter solution was preheated to the reaction temperature and rapidly added to the reactor. The resulting reaction mixture (approximately 40 mL) was vigorously stirred by a magnetic bar at 800 rpm.

A known amount of reaction mixture (*ca.* 0.5 g) was sampled at different reaction times and was analysed by HPLC, using a known amount of a 30 mg g<sup>-1</sup> aqueous solution of oxalic acid as an internal standard (*ca.* 15 mg of oxalic acid was added to each aliquot). Subsequently, the aliquot was diluted 10–20 times with water. This diluted aliquot, after being filtered through a 0.22 µm syringe filter, was then analysed in an Agilent 1200 HPLC chromatograph equipped with a refraction index detector and a Bio-Rad Aminex HPX-87H column (300 mm × 7.8 mm). A 0.005 M H<sub>2</sub>SO<sub>4</sub> mobile phase was employed as the eluent at 328 K and a 0.4 mL min<sup>-1</sup> flow rate. In addition to oxalic acid and furfural, the following products were detected by HPLC: MA, malic acid, SA, formic acid (FA), fumaric acid (FumA), 5-hydroxy-furan-2(5*H*)-one (hydroxyfuranone), furan-2(5*H*)-one (furanone) and furoic acid (FurA). Deeper details of the analyses are given in Fig. SI1 of ESI section.†

Furfural conversion and product yields were calculated according to the following formulas:

$$\text{Furfural conversion (mol\%)} = \frac{m_{\text{furf}}^0 - m_{\text{furf}}}{m_{\text{furf}}^0} \times 100$$

$$\text{Product yield (mol\%)} = \frac{m_{\text{prod}}}{m_{\text{furf}}^0} \times 100$$

where  $m_{\text{furf}}^0$  refers to the mole quantity initially loaded into the reactor, and  $m_{\text{furf}}$  and  $m_{\text{prod}}$  refer to the number of moles of the furfural and products, respectively, in the reaction mixture at a given time. The HPLC chromatographic factor of the organic products was calculated by analysing solutions with known concentrations of the different organic products.

The hydrogen peroxide concentration at a given reaction time was determined by iodometric titration. Approximately 0.5 g of reaction sample was diluted 10–20 times with water. Then, 0.5 g of this diluted solution was poured into an Erlenmeyer flask containing 20 mL of water. After adding 2 mL of potassium iodide solution (10%) and 2.5 mL of an acid mixture consisting of a solution of ammonium molybdate and H<sub>2</sub>SO<sub>4</sub>, the flask was closed, gently agitated and allowed to rest for five minutes to form triiodide species by oxidation of the iodide with H<sub>2</sub>O<sub>2</sub>, which gives a brown colour to the solution. The

mixture was then titrated with a *ca.* 0.1 M sodium thiosulfate solution until the brown triiodide colour was reduced to a light straw colour. A few drops of starch solution (10 g L<sup>-1</sup>) were added, and the solution became dark blue. Titration was continued until the colour of the solution changed sharply from blue to colourless. A titration of a blank solution (pure water) was also carried out following the same procedure. The actual titer of the sodium thiosulfate solution was determined by titration with potassium iodate solution (0.1 N).

The amount of H<sub>2</sub>O<sub>2</sub> present in solution was calculated as follows:

$$\begin{aligned} &\text{H}_2\text{O}_2 \text{ present in reaction mixture (mol)} \\ &= (A - B)(M) \frac{1 \text{ mol H}_2\text{O}_2}{2 \text{ mol Na}_2\text{S}_2\text{O}_3} \frac{34}{1 \text{ mol H}_2\text{O}_2} \end{aligned}$$

where  $A$  is the titration volume of Na<sub>2</sub>S<sub>2</sub>O<sub>3</sub> for the sample,  $B$  is the titration volume of Na<sub>2</sub>S<sub>2</sub>O<sub>3</sub> consumed for the blank and  $M$  is the molarity of the Na<sub>2</sub>S<sub>2</sub>O<sub>3</sub> solution.

For the reutilisation tests, catalyst was filtered out of the reaction medium by using a filtration cell and a ceramic membrane. The catalyst was washed twice with water (*ca.* 200 mL) to remove reaction products that could interfere in successive analysis, carefully removed from the membrane to prevent losses during handling, and dried at 333 K overnight before performing a new reaction run. The filtered solution from the catalyst wash steps (including the filtrate from the reaction medium) was analysed by TXRF for the quantitative determination of Ti and Si.

### Catalyst characterisation

Powder X-ray diffraction (XRD) measurements were performed at room temperature in the 5–50° range in scan mode (0.02°, 1 s) with a Siemens D5000 automated diffractometer, over a 2θ Bragg–Brentano geometry using Cu Kα radiation and a graphite monochromator.

Nitrogen adsorption–desorption isotherms were recorded at the temperature of liquid nitrogen (77 K) using a Micromeritics TriStar 3000 apparatus. The sample was previously outgassed at 140 °C for several hours. The specific area was calculated by applying the BET method to the range of relative pressures ( $P/P^0$ ) of the isotherms between 0.03 and 0.3 and by assuming a value of 0.162 nm<sup>2</sup> for the cross-section of adsorbed nitrogen molecules at 77 K.

TXRF (total reflection X-ray fluorescence) analysis was performed in a S2 PICOFOX instrument equipped with two X-ray fine focus lines, Mo and W anodes, and a Co(Li) detector with an active area of 80 mm<sup>2</sup> and a resolution of 157 eV at 5.9 keV (Mn Kα). The acquisition time was 300 s and 500 s for qualitative and quantitative analysis, respectively. To carry out the TXRF analysis, a Mo X-ray source was used for Si and Ti determination. For the analysis of solid samples, 10–15 mg of sample was ground in an agate mortar to a powder with a particle size less than 10 µm. Subsequently, 10 mL of high-purity water was added to the powder. The sample was homogenised for 15–20 min by ultrasonic desegregation in order to disperse any possible agglomeration of particles. A 5 µL aliquot of the

suspension was removed and placed on a flat carrier of plastic after which the water was evaporated by vacuum.

Raman spectra were recorded on a single-monochromator Renishaw 1000 spectrophotometer equipped with a CCD cool detector (200 K), with an argon laser as the exciting source ( $\lambda = 532$  nm), a supernotch filter, and an *in situ* cell that enables sample treatment under a flow of gas. Raman spectra were recorded at room temperature with a laser power of 2 mW after an *in situ* calcination of the samples in synthetic air with a heating rate of  $10\text{ K min}^{-1}$  up to 833 K for 30 min.

X-ray photoelectron spectra (XPS) were acquired with a VG Escalab 200 R spectrometer equipped with a hemispherical electron analyser and a Mg K $\alpha$  (1253.6 eV) X-ray source. The solids were outgassed at 393 K for 1 h at  $10^{-5}$  mbar to remove water before transfer to the ion-pumped analysis chamber. Ti 2p, C 1 s, O 1 s and Si 2p core level were scanned a sufficient number of times to obtain high signal-to-noise ratios. The static charge of the samples was corrected by referencing all binding energies (BEs) to the Si 2p peak (103.4 eV). The accuracy of the BE was  $\pm 0.1$  eV. The areas of the peaks were computed by fitting the experimental spectra to Gaussian/Lorentzian curves after removing the background (using the Shirley function). Surface atom ratios were calculated from peak area ratios normalised by using the corresponding atomic sensitivity factors.<sup>28</sup>

Thermogravimetric analysis (TGA) under a controlled atmosphere was carried out on a Mettler Toledo TGA/SDTA 851<sup>e</sup>, using a heating rate of  $10\text{ K min}^{-1}$  up to a maximum temperature of 973 K under a synthetic air atmosphere.

## Results and discussion

### Parametric study of the reaction conditions

A study of the effect of different operating variables on catalytic behaviour was performed first. The aim was to find the best reaction conditions to obtain the highest MA yield. The following operation variables were modified: reaction temperature,  $\text{H}_2\text{O}_2$  and furfural concentrations and catalyst loading.

**Reaction temperature effect.** The effect of reaction temperature on the catalytic properties was examined first. Temperatures in the range used for other catalysts were explored.<sup>15–19</sup> Fig. 1 compares the catalytic activity of commercial TS-1 at three different temperatures (323, 333 and 343 K) while keeping the rest of the reaction conditions constant (4.6 wt% of furfural, 2.3 wt% of catalyst and 12.3 wt%  $\text{H}_2\text{O}_2$ , equivalent to an  $\text{H}_2\text{O}_2$ /furfural mol ratio of 7.5). Yields are based on the initial amount of furfural loaded into the reactor.

5-Hydroxy-furan-2(5*H*)-one (hydroxyfuranone), MA and FA were the main reaction products, malic acid was also detected but with a yield less than 5%. The yield for the remaining possible reaction products (SA, furanones, FumA, furoic acid) was well below 2.4%. The low yield of these products, especially SA and furanones, was rather unexpected: previous results obtained in the liquid phase oxidation of furfural with  $\text{H}_2\text{O}_2$  yielded a wider variety of products including SA and furanones.<sup>15–19</sup> It is concluded that the reaction mechanism when using TS-1 is different to that of the conventional acid catalysts used previously to conduct this reaction. When acid catalysts

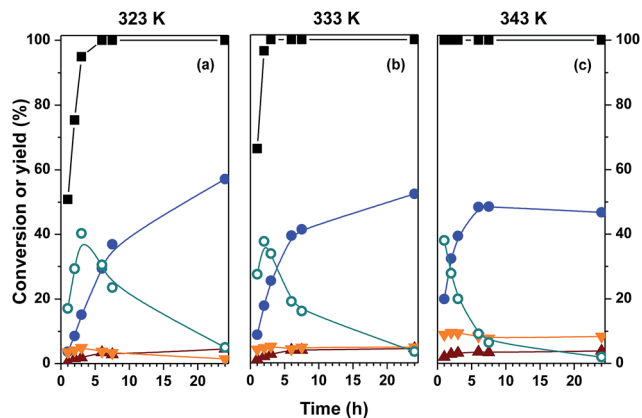


Fig. 1 Effect of reaction temperature on the catalytic properties of TS-1 at three different temperatures: (a) 323 K, (b) 333 K and (c) 343 K. Reaction conditions: 4.6 wt% of furfural, 2.3 wt% of catalyst, 12.3 wt% of  $\text{H}_2\text{O}_2$ , equivalent to a  $\text{H}_2\text{O}_2$ /F mol ratio = 7.5. Symbols: furfural conversion (■); 5-hydroxy-furan-2(5*H*)-one yield (○); maleic acid yield (●); formic acid yield (▼); and malic acid yield (▲).

are used, the reaction initiates with a Bayer–Villiger step to form 2-hydroxyfuran, which is in equilibrium with furan-2(5*H*)-one and furan-2(3*H*)-one (see Scheme SI1†). The eventual oxidation of these furanones gives rise to SA, hydroxyfuranone and MA. Therefore, it appears that when reaction initiates with a Baeyer–Villiger oxidation, a wider distribution of products is obtained.<sup>15–19</sup> This is not the case with TS-1. We will return to these points when discussing the reaction mechanism below.

It was also assumed that formic acid arises both from the deep oxidation of the organics and from the loss of formic acid required to convert a  $\text{C}_5$  chemical into a  $\text{C}_4$  compound.<sup>19</sup> Accordingly, the FA yield was calculated by subtracting the FA supposedly released by the formation of  $\text{C}_4$  products (1 mol of FA per mol of  $\text{C}_4$  product) from the total molar quantity of FA detected (the molar quantity of FA formed by deep oxidation was divided by 5 to express the value on a furfural basis). As shown in further figures, the carbon balance can approach 100% under optimum reaction conditions, but for the reaction conditions used in Fig. 1, the carbon balance was always below 100%. In principle, this incomplete carbon balance may be due to the total oxidation to  $\text{CO}_2$  (not quantifiable by HPLC analysis). However, this is not the only possibility, and the formation of HPLC-silent products can also contribute to the incomplete carbon balance. The carbon balance improved as the reaction progressed, suggesting that these unidentified HPLC products may be (partially oxidised) intermediates of the reaction.

As expected, the rate of furfural conversion increased upon raising the reaction temperature. Thus, at 323 K, full furfural conversion was reached after 6 h, whereas only 3 h was required for 333 K and 1 h was enough at 343 K. A rapid perusal of the figures also indicates that at short reaction times, hydroxyfuranone predominates among the detected products, but for longer periods, MA is the major product. It has been previously suggested that MA is formed at the expense of hydroxyfuranone oxidation; in our experiments at 323, 333 and 343 K, the hydroxyfuranone yield reached a maximum (close to 40%) at 3,



2 and 1 h, respectively, while MA yield continuously rose, indicating that the latter is not a primary product.<sup>19</sup> A remarkable result is that the maximum yield of MA (57%) was achieved at 323 K after 24 h of reaction, whereas at higher reaction temperatures, the yield decreased. Thus, the maximum yield at 333 K was 52% (for 24 h), and the maximum at 343 K was 49% (for 6 h). For longer reaction times at 343 K, the MA yield visibly decreased.

In a reaction pathway compatible with the results of Fig. 1, furfural is rapidly oxidised through unknown intermediates to hydroxyfuranone: a C<sub>1</sub> species (formic acid) is released to form the C<sub>4</sub> product. Hydroxyfuranone is subsequently oxidised to MA. In addition, furfural and all the other organic products can undergo deep oxidation to formic acid and to CO<sub>2</sub>.

In summary, for the reaction temperatures tested, 323 K results in the maximum MA yield. This was the reaction temperature selected for further studies. We discarded lower temperatures because the reaction rates would be very slow. Similar conclusions can be reached by working at lower H<sub>2</sub>O<sub>2</sub> concentrations at the three different temperatures tested (results included in Fig. SI2 of the ESI†).

**H<sub>2</sub>O<sub>2</sub> concentration effect.** Fig. 2 shows the effect of hydrogen peroxide concentration on the catalytic properties. Three different H<sub>2</sub>O<sub>2</sub> concentrations were tested (6.6, 12.3 and 24.6 wt%), equivalent to H<sub>2</sub>O<sub>2</sub>/furfural mol ratio of 4, 7.5 and 15, respectively. The remaining reaction parameters were kept constant (4.6 wt% of furfural, 2.3 wt% of catalyst and 323 K). The hydrogen peroxide concentration was in excess of the stoichiometric amount required for the oxidation of furfural to MA, which is H<sub>2</sub>O<sub>2</sub>/MA (mol mol<sup>-1</sup>) = 3. The larger the H<sub>2</sub>O<sub>2</sub> concentration, the faster the furfural conversion rate. For the highest H<sub>2</sub>O<sub>2</sub>/furfural mol ratio tested, which was 15, full furfural conversion was attained in just 2 hours of reaction, whereas 3 h was needed for H<sub>2</sub>O<sub>2</sub>/furfural mol ratio = 4.

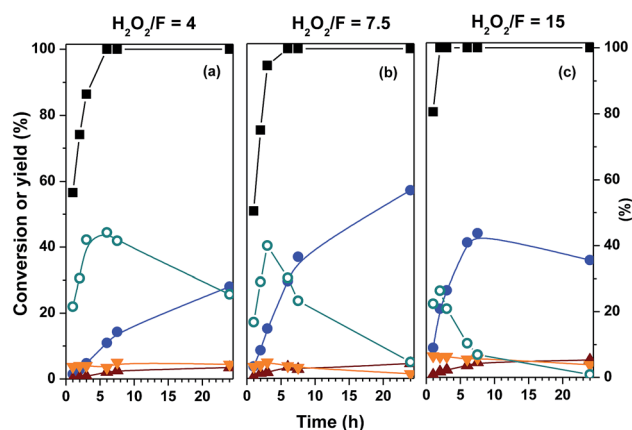


Fig. 2 Effect of H<sub>2</sub>O<sub>2</sub> concentration on the catalytic properties of TS-1 for three different H<sub>2</sub>O<sub>2</sub>/furfural mol ratios (4, 7.5 and 15), corresponding to (a) 6.6, (b) 12.3 and (c) 24.6 wt% of H<sub>2</sub>O<sub>2</sub>. Reaction conditions: 4.6 wt% furfural, 323 K, 2.3 wt% catalyst. Symbols: furfural conversion (■); 5-hydroxy-furan-2(5H)-one yield (○); maleic acid yield (●); formic acid yield (▼); and malic acid yield (▲).

As regards the transformation to oxidised C<sub>4</sub> compounds, the major detected products were hydroxyfuranone and maleic acid; the combined yield of FA and malic acid was smaller than 9%. The yields of the remaining products was smaller than 2%. For H<sub>2</sub>O<sub>2</sub>/furfural mol ratio = 4, the MA formation rate was slower than that at 7.5; thus, after 24 h of reaction, only a 28% MA yield was reached, whereas for a ratio of 7.5, the yield was 57%. In principle, one might assume that a H<sub>2</sub>O<sub>2</sub>/furfural mol ratio > 7.5 would result in a better MA yield, and at short reaction times (time < 7.5 h) in these conditions, the formation rate of MA is substantially faster (at the expense of a faster disappearance of hydroxyfuranone). However, the MA yield attains a maximum yield of 44% at 7.5 h of reaction, and after 24 h of reaction it decreases to 36%. The high hydrogen peroxide concentration results in an overoxidation of MA.

In summary, an excess of H<sub>2</sub>O<sub>2</sub> with respect to the stoichiometric amount for furfural oxidation to MA is needed to improve the MA yield. The optimum H<sub>2</sub>O<sub>2</sub>/furfural mol ratio is approximately 7.5; lower ratios result in lower reaction rate, and larger ratios result in overoxidation. Similar conclusions were obtained when conducting similar experiments to those presented in Fig. 2, but with a larger catalyst concentration (4.6 wt%). The results are presented in Fig. SI3 of the ESI section.†

**Catalyst loading effect.** The effect of catalyst loading on catalytic properties is depicted in Fig. 3: experiments were conducted by changing the catalyst concentration and keeping constant the reaction temperature (323 K), the furfural concentration (4.6 wt%), and the H<sub>2</sub>O<sub>2</sub> concentration (12.3 wt%, H<sub>2</sub>O<sub>2</sub>/furfural mol ratio = 7.5). When no catalyst was incorporated, the furfural conversion rate was lower than when catalysed with TS-1; SA and furan-2(5H)-one were the major products detected; FumA and FurA were also observed but with a yield lower than 4 and 6%, respectively; and the MA yield was negligible except at 24 h of reaction. This behaviour is compatible with a self-catalysed reaction, following a reaction mechanism in which the first step is the Baeyer-Villiger oxidation of furfural to 2-hydroxyfuran. A similar situation was found for other experiments conducted without TS-1 catalyst but with lower and higher H<sub>2</sub>O<sub>2</sub> concentrations: SA and furan-2(5H)-one were the major products (see Fig. SI4 in the ESI†). The addition of 1.2 wt% of catalyst substantially accelerated the furfural conversion rate and, more importantly, remarkably modified the yield pattern of the obtained products: the yields of SA and furanone significantly decreased and became negligible, whereas MA and hydroxyfuranone were the major products.

The incorporation of more catalyst intensifies this effect, and thus, for a catalyst concentration of 4.6 wt% (TS-1/furfural wt. ratio = 1), a MA selectivity close to 80% was attained for 24 h of reaction, with residual formation of malic and formic acids. It must be stressed that, for the latter specific reaction conditions, the carbon balance was close to 100% for all aliquots analysed throughout the kinetic experiments. The latter suggests that for a catalyst concentration lower than 4.6% a carbon balance smaller than 100% would be very likely due to the formation of undetectable intermediates. On the other hand, a larger catalyst concentration (9.2 wt%) resulted in the overoxidation of MA,

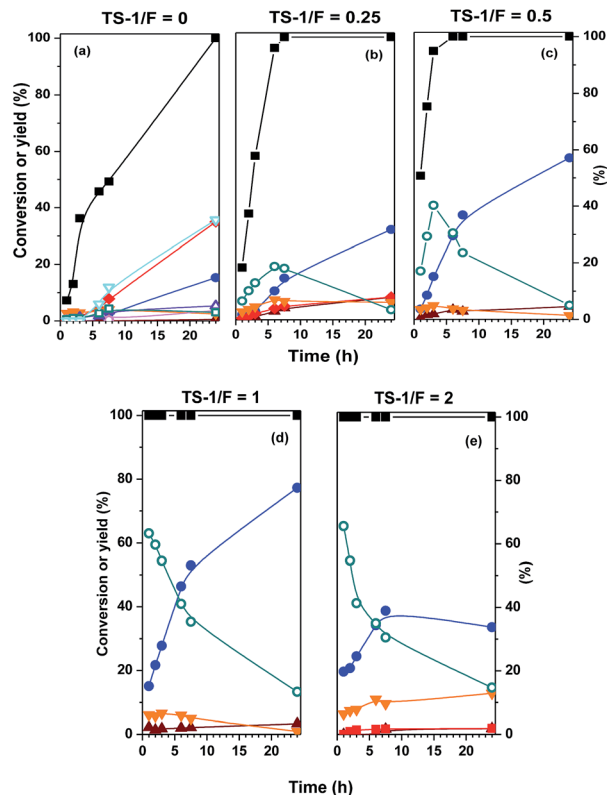


Fig. 3 Effect of catalyst loading (wt%) on the catalytic properties of TS-1: (a) 0 wt%; (b) 1.2 wt%; (c) 2.3 wt%; (d) 4.6 wt%; (e) 9.2 wt%. Reaction conditions: 4.6 wt% furfural, 323 K and  $\text{H}_2\text{O}_2/\text{F}$  = 7.5, which correspond to 12.3 wt%  $\text{H}_2\text{O}_2$ . Symbols: furfural conversion (■); 5-hydroxy-furan-2(5H)-one yield (○); maleic acid yield (●); formic acid yield (▼); malic acid yield (▲); furan-2(5H)-one yield (▽); succinic acid yield (◆).

very likely to  $\text{CO}_2$ , as can be deduced from the lower MA yield, larger FA yield and incomplete carbon balance.

**Effect of concentration of furfural in aqueous solution.** Fig. 4 shows the effect of furfural concentration on conversion and yields; the reaction temperature,  $\text{H}_2\text{O}_2/\text{furfural}$  mol ratio and TS-1/furfural wt ratio were kept constant at 323 K, 7.5 and 1, respectively. In this figure, the conversion and selectivity of  $\text{H}_2\text{O}_2$  during the course of the reaction is also included.  $\text{H}_2\text{O}_2$  conversion % indicates the ratio of the total  $\text{H}_2\text{O}_2$  consumed to the initial  $\text{H}_2\text{O}_2$  loaded, whereas the selectivity is the ratio of the mol% of  $\text{H}_2\text{O}_2$  consumed to produce the  $\text{C}_4$  organic compounds detected by HPLC analysis to the mol% of  $\text{H}_2\text{O}_2$  actually consumed (the amount theoretically consumed to produce FA is not included in this quantity). Except for the experiment conducted with 9.2 wt% of furfural, the carbon balance was essentially well above 90% in all experiments. This indicates that most of the organic products were detected by HPLC in this series of experiments, and consequently, the deviation of the  $\text{H}_2\text{O}_2$  selectivity from 100% is an indication of the unselective conversion (decomposition) of  $\text{H}_2\text{O}_2$ .

$\text{H}_2\text{O}_2$  consumption is very selective at the beginning of the reaction when hydroxyfuranone predominates. However, as the reaction proceeds, selectivity worsens, indicating that a large fraction of  $\text{H}_2\text{O}_2$  is consumed in unselective transformations.

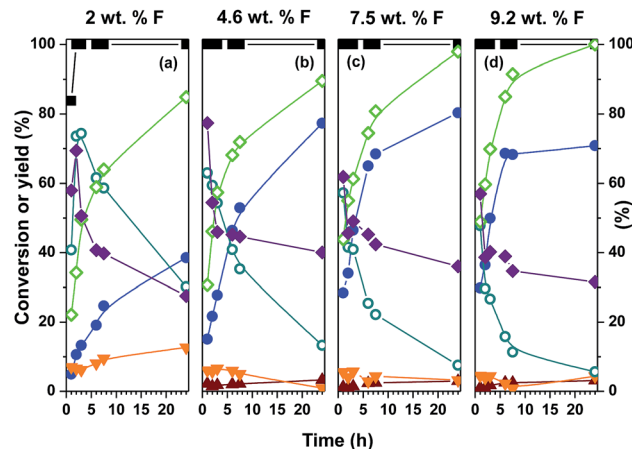


Fig. 4 Effect of furfural concentration (wt%) on the catalytic behaviour of TS-1: (a) 2 wt%; (b) 4.6 wt%; (c) 7.5 wt%; and (d) 9.2 wt% of furfural. Reaction conditions: 323 K, TS-1/F wt ratio = 1;  $\text{H}_2\text{O}_2/\text{F}$  mol ratio = 7.5. Symbols: furfural conversion (■); 5-hydroxy-furan-2(5H)-one yield (○); maleic acid yield (●); formic acid yield (▼); malic acid yield (▲); furan-2(5H)-one yield (▽); succinic acid yield (◆);  $\text{H}_2\text{O}_2$  conversion (◇);  $\text{H}_2\text{O}_2$  selectivity (♦).

Thus, when 4.6 wt% of furfural is used (Fig. 4b), for 1 h of reaction, the selectivity of the  $\text{H}_2\text{O}_2$  devoted to produce  $\text{C}_4$  compounds is close to 80%, and as the reaction progresses, the selectivity continuously decreases down to a value of 40% after 24 h of reaction. Similar trends can be observed for the remaining experiments in Fig. 4. Formic acid formation partly explains the unselective transformation of  $\text{H}_2\text{O}_2$ , but there are other unselective routes; we will address this point in Section 3.3.

Regarding MA selectivity, a very remarkable result is that for reaction times shorter than 7.5 h, the furfural concentration clearly has a very positive effect on the MA yield. Thus, the MA yield after 7.5 h of reaction is 25, 53, 68 and 69% for 2, 4.6, 7.5 and 9.2 wt% of furfural, respectively. The intrinsic MA formation rate was calculated after 1 h of reaction to take into account the fact that the catalyst concentration also increases throughout the series of experiments (furfural/TS-1 ratio was kept constant). The intrinsic rate was found to be 0.14, 0.44, 0.82 and 0.87  $\mu\text{mol}$  of furfural  $\text{g}_{\text{cat}}^{-1} \text{s}^{-1}$  for 2, 4.6, 7.5 and 9.2 wt% of catalyst, respectively. Therefore, the intrinsic MA reaction rate also rises with furfural concentration, which means that the effect is due to the increase of furfural concentration. An explanation could be that as the furfural concentration rises, so does the relative surface furfural coverage with respect to other reactants. In any case, the increase in both the MA yield and formation rate levels off for furfural concentrations larger than 7.5 wt%. Moreover, when 9.2 wt% of furfural is used, overoxidation of MA is evident for longer reaction times; thus, for 24 h of reaction, the MA yield (71% yield) is smaller than that for the 4.6 and 7.5 wt% experiments (78 and 80% yields, respectively). The overoxidation of products in the 9.2 wt% experiment is also evident by the stronger deviation of the carbon balance, to a value notably lower than 100%.

In summary, we can conclude that among all the reaction conditions tested, the optimum reaction conditions to obtain

the highest MA yield (80%) are those used in Fig. 4b and c: 323 K, between 4.6–7.5 wt% of TS-1, TS-1/furfural wt ratio = 1;  $\text{H}_2\text{O}_2$ /furfural mol ratio = 7.5 and 24 h of reaction.

### Comparison with other solid catalysts and reaction mechanisms

Fig. 5 compares the catalytic behaviour of TS-1 with other selected catalysts. Reaction conditions, indicated in the caption, were selected to obtain a high MA yield with TS-1. Ambelyst 70, a sulphonic resin, was chosen because of its proven capacity to catalyse furfural oxidation to  $\text{C}_4$  diacids.<sup>15,16,19</sup> ZSM-5, a Ti-free zeolite with acid sites, was tested because it presents the same MFI-like silica framework as TS-1. Finally, anatase, which has also been detected to be present in the TS-1 as a result of deficient insertion of Ti within the MFI-like framework, was also investigated.

Amberlyst 70 displayed an oxidation activity pattern typically catalysed by strong acids and a wide number of products can be obtained.<sup>15,16,19</sup> Succinic acid, furan-2(5H)-one and maleic acid are mainly formed, hydroxyfuranone, and malic, fumaric and formic acids are also detected at non-negligible yields, especially at shorter reaction times. After 24 h of reaction, the yield of SA, furan-2(5H)-one and MA was approximately 50, 30 and 20%, respectively. Although the ZSM-5 zeolite presents acid sites on its surface, these sites are not as active as those of TS-1 or as the sulphonic sites of Amberlyst 70. The latter presents a comparatively large strong-acid-site concentration ( $2.55 \text{ mmol g}_{\text{cat}}^{-1}$ ),<sup>19</sup> which explains its relatively high activity. ZSM-5 displays an activity pattern resembling that of a catalyst-free run (see Fig. 3a). After 24 h of reaction, an MA yield of 15% and SA yield of 30% was observed for ZSM-5. Accordingly, the catalytic activity of TS-1 cannot be associated to acid sites present in the MFI-framework of TS-1, but rather to the presence of Ti(IV) sites in the TS-1. Anatase presents very active sites,

but the Ti sites in anatase are not as selective as framework Ti in TS-1: the  $\text{H}_2\text{O}_2$  efficiency is lower, the carbon balance is incomplete and the MA yield is lower (MA yield of 31% was observed after 24 h of reaction). These latter results suggest that Ti sites in anatase are not responsible for the good behavior of TS-1. In summary, among the family of catalysts tested, TS-1 features a high activity and selectivity to MA.

**A proposal of the reaction mechanism for oxidation using TS-1 catalyst.** The first characteristic of the performance of TS-1 is the low selectivity for succinic acid and furan-2(3H)-one with respect to values obtained with sulphuric acid, sulphonic resins or poly(styrene sulphonic acid).<sup>15–18,29</sup> This strongly suggests that the reaction with TS-1 goes through a different mechanism. It is accepted that, when using catalysts possessing sulphonic acid sites, the reaction starts with a Baeyer–Villiger step (see Scheme SI1†). Fig. SI6† and the discussion therein demonstrate that, when using TS-1, furfural oxidation does not start with a Baeyer–Villiger oxidation.

It has been reported that furan can be oxidised very selectively with hydrogen peroxide to maleic dialdehyde<sup>21</sup> or to hydroxyfuranone<sup>22</sup> by using a  $\text{H}_2\text{O}_2$ /furfural mol ratio of 1 and 2, respectively. The latter can eventually be oxidised to MA. Therefore, if furan could be formed from furfural, the oxidation of furan would yield MA, provided that a  $\text{H}_2\text{O}_2$ /furfural ratio > 2 is used.

One possibility is that the reaction starts with the oxidation of furfural to furoic acid, which can subsequently be transformed to furan by releasing formic acid (see Scheme SI2 in the ESI† for a description of this mechanism proposal). However, this possibility can be discarded because when the oxidation of furoic acid with  $\text{H}_2\text{O}_2$  was conducted by using TS-1 (at 323 K, 4.6 wt% of furoic acid, 4.6 wt% of TS-1 and a  $\text{H}_2\text{O}_2$ /furoic acid mol ratio of 7.5, equivalent to 12.3 wt%) the MA yield was much lower than that obtained with furfural (see Fig. SI7 in the ESI† for further details).

Another plausible possibility is that furan can be formed by the decarbonylation of furfural. However, the decarbonylation of furfural requires different catalysts and reaction conditions to proceed,<sup>30–32</sup> and therefore this route can also be discarded.

We propose a different mechanism based on the results and on the proposal of Jacobs *et al.* when oxidising furan to maleic dialdehyde.<sup>21</sup> They proposed that one of the double bonds in the furan ring is epoxidised and the thus-formed epoxide then rapidly rearranges, yielding unsaturated 1,4-dicarbonyl compounds. The same epoxidation and rearrangement steps can be applied to furfural (see Scheme 1): the double bond with less steric hindrance is selectively epoxidised, and the furfural-epoxide rapidly undergoes a rearrangement to yield the Z-4-oxopent-2-enal. The loss of a carbon atom is still needed for the formation of the corresponding  $\text{C}_4$  derivative. We propose that the formation of a  $\text{C}_4$  intermediate occurs *via* Baeyer–Villiger oxidation of the aldehyde functionality at 1-position of the Z-4-oxopent-2-enal. An ester is formed, which is rapidly hydrolysed to form  $\beta$ -formylacrylic acid ((Z)-4-oxobuten-2-enoic acid), releasing formic acid. The electron withdrawing nature of the acyl group directly bonded to the reacting aldehyde at C1 strongly increases its electrophilicity favoring the Baeyer–

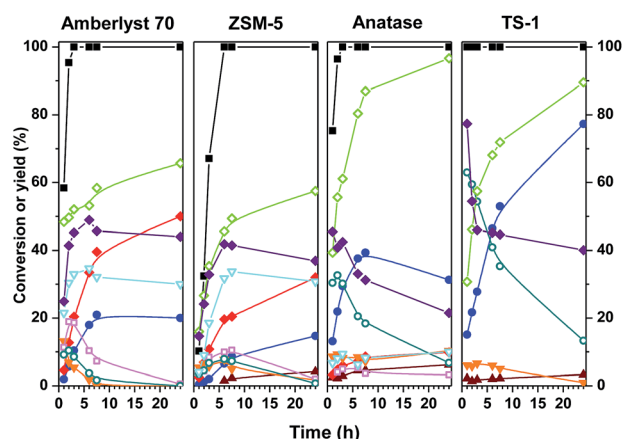
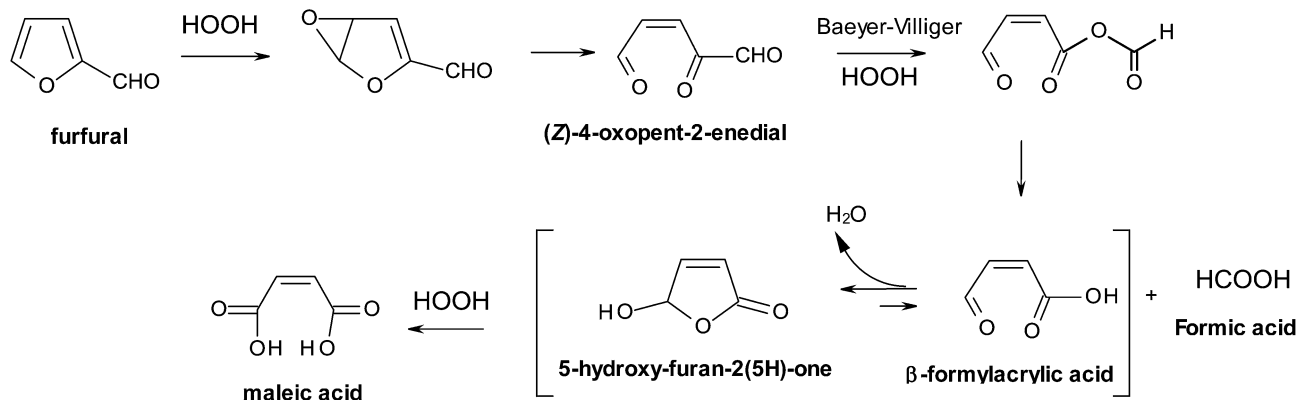


Fig. 5 Catalytic activity of the different catalysts tested: (a) Amberlyst 70; (b) ZSM-5; (c) Anatase; and (d) TS-1. Reaction conditions: 4.6 wt% furfural, 4.6 wt% catalyst, 323 K,  $\text{H}_2\text{O}_2/\text{F} = 7.5$ , which corresponds to 12.3 wt%  $\text{H}_2\text{O}_2$ . Symbols: (■) furfural conversion; 5-hydroxy-furan-2(5H)-one yield (○); maleic acid yield (●); formic acid yield (▼); malic acid yield (▲); furan-2(5H)-one yield (▽); succinic acid yield (◆); fumaric acid yield (□);  $\text{H}_2\text{O}_2$  conversion (◇);  $\text{H}_2\text{O}_2$  selectivity (◆).



Scheme 1 Proposal of mechanism via epoxidation of the furan ring and subsequent release of formic acid.

Villiger reaction and justifying the regioselectivity of the process. Formylacrylic acid is in equilibrium with the hydroxyfuranone. Experimentally, the formation of MA parallels the consumption of hydroxyfuranone. This suggests that hydroxyfuranone can be directly oxidised to MA. However, it cannot be excluded that MA is formed by the oxidation of  $\beta$ -formylacrylic, in equilibrium with hydroxyfuranone. We could not identify any HPLC peak as  $\beta$ -formylacrylic, very likely because the equilibrium is strongly shifted to hydroxyfuranone. It is also possible that the former is present at very low concentration, and therefore difficult to detect by HPLC, but still involved as an intermediate of the reaction. If so, whereas  $\beta$ -formylacrylic is consumed by oxidation to MA, so must be hydroxyfuranone.

### Improvement in selective utilisation of H<sub>2</sub>O<sub>2</sub> using a two-step process

In principle, there are three routes to convert H<sub>2</sub>O<sub>2</sub>: conversion to organic products (including formic acid), catalytic decomposition and uncatalysed thermal decomposition. Blank experiments (see Fig. S15 in the ESI† and discussion therein) allowed us to conclude that (i) although TS-1 catalytically decomposes H<sub>2</sub>O<sub>2</sub>, the decomposition is remarkably inhibited by the presence of furfural, especially at short reaction times and (ii) thermal decomposition is less than 20% after 24 h of reaction. This has practical implications when searching for further improvements in the selective utilisation of hydrogen peroxide: first, catalytic decomposition is very low at short reaction times, and second, the thermal decomposition of H<sub>2</sub>O<sub>2</sub> is as important as catalytic decomposition.

The stoichiometric H<sub>2</sub>O<sub>2</sub>/furfural mol ratio required to selectively oxidise furfural to MA is 3. The maximum yield to MA was achieved by using a mol ratio = 7.5, which is more than double the stoichiometric ratio. The unselective utilisation of H<sub>2</sub>O<sub>2</sub> comes from thermal and catalytic decomposition. Interestingly, the results presented in Fig. S15† indicate that the catalytic decomposition is seriously inhibited by the presence of furfural. At the beginning of the reaction, decomposition is practically negligible: only after 5 hours is the catalytic decomposition detectable.

On the other hand, when TS-1 is used as catalyst and at short reaction times, hydroxyfuranone is primarily produced, with a relatively selective utilisation of H<sub>2</sub>O<sub>2</sub>. Kinetic data show that furfural oxidation to hydroxyfuranone is very rapid and selective, even when lower H<sub>2</sub>O<sub>2</sub>/furfural mol ratios are used (see Fig. S13a†). Therefore, a good strategy would be to conduct the oxidation in two steps; in the first step, to oxidise rapidly furfural to hydroxyfuranone using TS-1 and a H<sub>2</sub>O<sub>2</sub>/furfural mol ratio close to stoichiometry. For short reaction times, the unselective catalytic decomposition of H<sub>2</sub>O<sub>2</sub> is prevented. In a subsequent step, the oxidation of hydroxyfuranone to MA will be conducted with another catalyst because TS-1 unselectively decomposes H<sub>2</sub>O<sub>2</sub>. Sulphonic-based catalysts have demonstrated a capacity to transform hydroxyfuranone to MA.<sup>15,16,19</sup>

In practice, we proceeded as follows: first, the oxidation of furfural to hydroxyfuranone was conducted by using TS-1 as catalyst with a H<sub>2</sub>O<sub>2</sub>/furfural mol ratio of 2.4 (2 mol of H<sub>2</sub>O<sub>2</sub> are needed for the stoichiometric oxidation of furfural to hydroxyfuranone). Previous reactions with a low H<sub>2</sub>O<sub>2</sub> concentration (Fig. S13a† (H<sub>2</sub>O<sub>2</sub>/F mol ratio = 2.15)) showed that after 4 hours of reaction, the hydroxyfuranone concentration did not increase, most likely because of the total consumption of the H<sub>2</sub>O<sub>2</sub>. For that reason, this first reaction step was carried out for 4 h. After that, the TS-1 catalyst was filtered off and the second oxidation step was conducted by using an Amberlyst 70 sulphonic resin as a catalyst. Further addition of H<sub>2</sub>O<sub>2</sub> was performed to obtain a H<sub>2</sub>O<sub>2</sub>/furfural mol ratio of 2 with respect to the initial furfural concentration. One mol of H<sub>2</sub>O<sub>2</sub> is needed for the stoichiometric oxidation of hydroxyfuranone to maleic acid, so a small excess of H<sub>2</sub>O<sub>2</sub> was incorporated to account for non-selective decomposition. To prevent the dilution of the reaction media, a 70 wt% H<sub>2</sub>O<sub>2</sub> solution was used to incorporate H<sub>2</sub>O<sub>2</sub> in this second step. Fig. 6 displays the results obtained by taking samples at different reaction times. Products yields are calculated with respect to the initially loaded furfural.

After 4 h, the oxidation of furfural with TS-1 resulted in a 70% hydroxyfuranone yield, while the yield of maleic acid was less than 10%. However, once the TS-1 was filtered off and Amberlyst 70 and further H<sub>2</sub>O<sub>2</sub> were incorporated, the selective



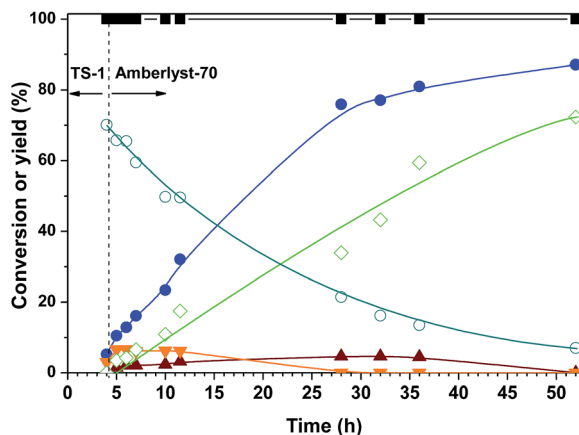


Fig. 6 Consecutive two-step oxidation of furfural with TS-1 and Amberlyst 70. Reaction conditions: 4.6 wt% furfural, 323 K and 4.6 wt% of catalyst for each step. Symbols: furfural conversion (■); 5-hydroxyfuran-2(5H)-one yield (○); maleic acid yield (●); formic acid yield (▼); malic acid yield (▲); and  $\text{H}_2\text{O}_2$  conversion (◇).

oxidation of hydroxyfuranone to maleic proceeded continuously, and after 24 h of reaction with Amberlyst (equivalent to 28 h of total reaction time), the MA yield was close to 76%, very close to that obtained after 24 h with TS-1 (78%). The MA yield reached almost 90% after 2 days with Amberlyst. These results therefore demonstrate that MA can be produced from furfural by a two-step catalyst process with high selective utilisation of both furfural and  $\text{H}_2\text{O}_2$ . The overall  $\text{H}_2\text{O}_2$ /furfural mol ratio was 4.4.

### Stability of the TS-1 catalyst

To evaluate the stability of the TS-1 catalyst in the oxidation of furfural, two different experiments were conducted. First, successive reutilisation runs were performed with aqueous solutions of pure furfural distributed by laboratory chemical suppliers. In another set of experiments, the stability of the catalysts was tested with furfural aqueous solutions obtained from biomass (corncoobs).

Regarding the aqueous solution of pure furfural, successive reutilisation runs were carried out after 7 h of reaction, with a catalyst and furfural content of 4.6 wt% and a  $\text{H}_2\text{O}_2$ /furfural molar ratio of 7.5, corresponding to 12.3 wt%  $\text{H}_2\text{O}_2$ . The catalyst was filtered off and dried before each new run (see Experimental section for details). Medium-term reaction times (7 h) are more sensitive to detect the deactivation processes. Longer reaction times may miss the deactivation if the deactivation is not very intense. Fig. 7 shows the results obtained after 6 reutilisation cycles. The conversion and the yields of the main products are represented (MA, 5-hydroxyfuranone and FA). The results of a blank experiment without TS-1 catalyst are also included (first column): much lower values for the conversion and yields to selective oxidation products were obtained in this blank test.

When TS-1 was reused, the conversion values remained at 100% throughout all the runs. Moreover, the yields of MA, hydroxyfuranone and formic acid remained quite similar for all the runs investigated; MA yields were between 43–48% and

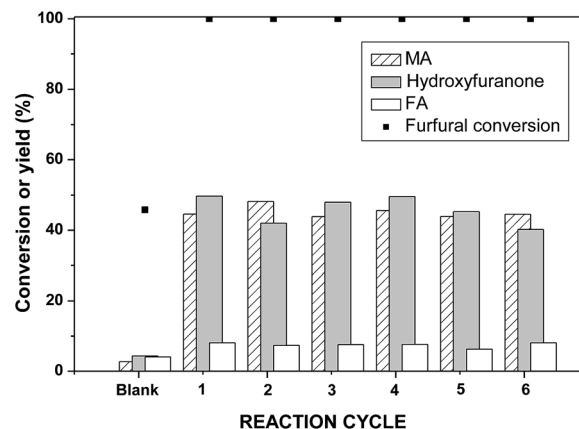


Fig. 7 TS-1 catalyst reutilisation tests for aqueous solution of furfural (4.6 wt%), 323 K,  $\text{H}_2\text{O}_2$ /F mol ratio = 7.5, corresponding to 6.6 wt% of  $\text{H}_2\text{O}_2$ , 4.6 wt% catalyst and 7 h reaction.

hydroxyfuranone between 40–50%. Attending to these results, we can conclude that when commercial furfural is used, TS-1 is quite stable, and no sign of deactivation could be observed for at least 6 cycles.

Reutilisation runs were also conducted by using aqueous furfural solutions obtained from lignocellulosic biomass. Briefly, furfural was obtained from corncoobs by using Amberlyst 70 as catalyst, at 453 K, 19 bar and by using a  $\text{N}_2$  flow of  $150 \text{ mL min}^{-1}$  (STP) to strip the water-furfural vapour stream. Stripping of furfural by  $\text{N}_2$  results in the rapid extraction of furfural from the reaction mixture, which prevents furfural from being consumed in further secondary reactions in the liquid phase. This furfural stream is condensed to separate gases from the aqueous furfural solution. Further details of the procedure can be found elsewhere.<sup>33,34</sup> The furfural concentration of this aqueous solution was determined to be 2.5% (GC analysis). Other impurities like acetic acid and 5-methyl-furfural were also detected by GC-MS. The results obtained after successive reutilisation runs at 323 K, 24 h of reaction,  $\text{H}_2\text{O}_2$ /furfural mol. ratio = 7.5 and catalyst/furfural wt ratio = 1 are displayed in Fig. 8. The actual furfural concentration in the reaction media was 2 wt%, and at this relatively low concentration of furfural, the rates of furfural conversion and MA formation are lower than those found when the optimum reaction conditions are set (see Fig. SI8 in the ESI† for the kinetics of oxidation when this biomass furfural solution was used, and see also Fig. 4a for the kinetic curve of commercial furfural at similar reaction conditions to those in Fig. 8). To obtain a measurable and relatively high MA yield (larger than 30%), a long reaction time is needed (24 h).

When aqueous furfural obtained directly from biomass is used, a slight but continuous deactivation of TS-1 can be observed. The deactivation is more visible in the MA yield, as the hydroxyfuranone yield remained above 40% for the first six runs (in the seventh run the yield dropped to 31%). It is also noteworthy that the formic acid yield slightly but inexorably increased upon reutilisation runs, which confirms that the selective oxidation sites of TS-1 are being deteriorated by the

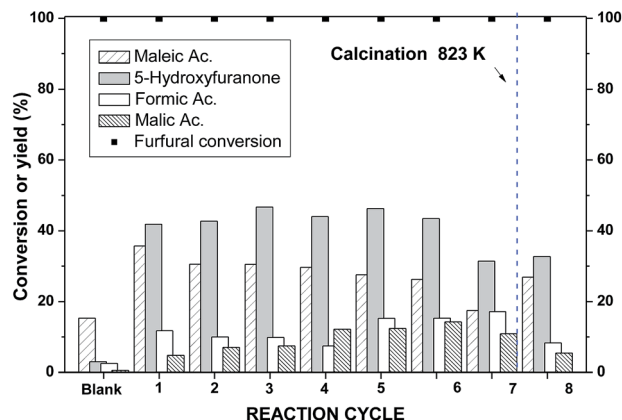


Fig. 8 Reutilisation experiments for aqueous furfural solution obtained from biomass. Reaction conditions: 2 wt% furfural, 323 K,  $\text{H}_2\text{O}_2/\text{F} = 7.5$ , which corresponds to 5.3 wt%  $\text{H}_2\text{O}_2$ , and 2 wt% catalyst, 24 h.

utilisation of real furfural. All these results strongly suggest that the impurities present in the real aqueous furfural derived from biomass have a detrimental effect on the deterioration of TS-1. The removal of these impurities from biomass-derived furfural aqueous solutions is recommended to prevent the deterioration of TS-1.

After the 7th run, the used TS-1 was filtered off, dried at 323 K overnight and finally calcined at 823 K in an oven under air for 3 hours. This calcined catalyst was again used for an additional 8th run, and the MA yield was partially restored. This indicates that the deactivation of TS-1 is partially due to the deposition of organic products derived from these impurities, which are removed by calcination. Other sources of deactivation will be discussed below.

These contaminants must be removed when considering an industrial application. As indicated in the Introduction, a double distillation is required to purify furfural.<sup>1</sup> The first distillation removes impurities and an azeotrope with 35% of furfural is yielded. The second distillation column further removes water and results in pure and very concentrated furfural.

The double distillation may compromise seriously the economic viability of the process here described. Possible solutions to reduce the cost and energy consumption can be the following. The azeotrope free of contaminants can be used for the oxidation to MA, preventing the use of the second distillation column. In practice the furfural–water azeotrope is condensed before entering the second vacuum distillation column and two phases are formed: a rich furfural phase (which is that readily further distilled) and a poorer aqueous furfural stream. Another solution could be that the latter diluted stream, free of contaminants, could be withdrawn and used in the oxidation to MA, leaving the concentrated furfural for processes requiring very concentrated and free of contaminants furfural.

### Characterisation of fresh and used catalyst

Fresh and used catalysts after several reaction cycles were characterised by different techniques with the intention of

identifying the possible physico-chemical changes occurring during utilisation. Laser Raman spectra of fresh and used catalyst samples using a 523 nm laser are represented in Fig. 9. The used catalyst after 6 runs with pure furfural is represented in Fig. 7. Samples were previously calcined *in situ* in the cell by flowing synthetic air at 823 K for 30 min. This treatment is required because hydrocarbonaceous species remain adsorbed on the catalyst after utilisation, which precludes the recording of good quality Raman spectra due to the fluorescence phenomenon associated with these C-containing residues (see Fig. S19 in the ESI†).

Raman bands at 290, 380, 437, 469, 815, 837, 960 and 1125  $\text{cm}^{-1}$  that have been previously reported for TS-1 are clearly observed in the Raman spectra of Fig. 9; the features at 960 and 1125  $\text{cm}^{-1}$  demonstrate the substitutional  $\text{Ti(IV)}$  insertion within the silica framework: they have been assigned to the stretching  $\text{Ti-O-Si}$  vibrations of inserted  $\text{TiO}_4$  tetrahedra (respectively, in-phase and out of phase antisymmetric stretching of the four connected  $\text{Ti-O-Si}$  bridges).<sup>35–38</sup> The bands detected at 144, 515 and 637  $\text{cm}^{-1}$  correspond to Raman features of anatase ( $\text{TiO}_2$ ); there must be another anatase-derived band at 390  $\text{cm}^{-1}$ , but it is overshadowed by the most intense band of TS-1 at 380  $\text{cm}^{-1}$ . Visible Raman spectroscopy is very sensitive to extraframework titanium oxide species and therefore is an excellent probe for the detection of very small  $\text{TiO}_2$  domains. Therefore, these bands demonstrate the presence of extraframework Ti and that not all the Ti cations are inserted within the zeolite framework.

No large differences can be detected between the spectra from fresh and used catalysts, which suggests that TS-1 is essentially unaltered by the utilisation of the catalyst in the reaction medium. Nevertheless, a closer examination (see inset in the figure) indicates that the  $\text{TiO}_2$  band at 144  $\text{cm}^{-1}$  is apparently less intense, which could suggest that there may be some leaching during the utilisation as catalyst.

Chemical analyses by TXRF were conducted to confirm the leaching. Ti and Si were analysed in both the fresh and used solids and in the liquid phase after each reaction run, the latter

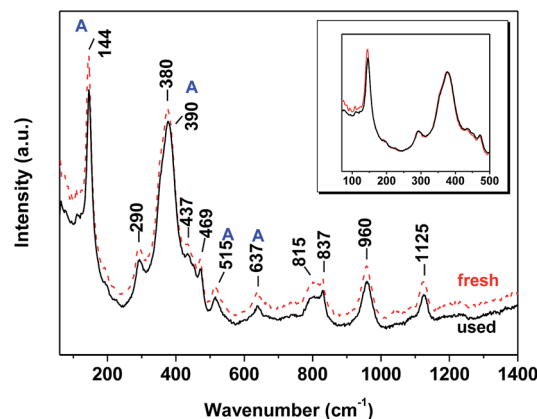


Fig. 9 Visible laser Raman spectra of fresh (dashed) and used (continuous) catalysts after *in situ* calcination at 823 K for 30 min in synthetic air. A denotes Raman bands from the anatase phase.

**Table 1** Summary of TXRF results of fresh and used catalysts and in the liquid reaction mixtures after successive reaction cycles

Catalyst	Si/Ti at. ratio in solid	Amount of metal leached to the reaction mixture (mg)							
			Run 1 <sup>b</sup>	Run 2 <sup>b</sup>	Run 3 <sup>b</sup>	Run 4 <sup>b</sup>	Run 5 <sup>b</sup>	Run 6 <sup>b</sup>	Run 7 <sup>b</sup>
Used with comm. furfural	31 (25.5) <sup>a</sup>	Ti	3.51 (11.2%)	0.96 (3%)	0.41 (1.3%)	0.47 (1.5%)	0.56 (1.8%)	0.36 (1.1%)	—
		Si	0.31 (0.03%)	0	0	0	0	0.27 (0.03%)	—
Used with biomass-derived furfural	29.4 (25.5) <sup>a</sup>	Ti	2.29 (15.4%)	0.46 (3.1%)	0.28 (1.9%)	0.28 (1.9%)	0.21 (1.4%)	0.24 (1.6%)	0.20 (1.3%)
		Si	0.48 (0.13%)	0.52 (0.14%)	0	0.31 (0.81%)	0.16 (0.04%)	0	0

<sup>a</sup> Si/Ti at. ratio of fresh sample. <sup>b</sup> Values between brackets represent the metal leached during the run cycle with respect to the total amount of metal initially present in the solid (expressed as wt%).

case for runs conducted with commercial and biomass-derived furfural. Table 1 summarises the results of TXRF.

The Si/Ti at. ratio of the catalyst used with the commercial furfural is clearly higher than that of fresh catalyst, which indicates that Ti was leached during the six utilisation runs. The same conclusion may be reached by examining the Ti concentration in the liquid reaction mixture. Most of the Ti is leached during the first run (*ca.* 56% of the total Ti leached), and the impact of lixiviation seems to decline upon reutilisation. Si leaching also takes place, although to a much smaller degree, and in some cases below the detection limit of the technique: Ti leaching represents *ca.* 20% of the initial Ti content, whereas Si leaching accounts for less than 0.1% of the initial Si.

The former TXRF analyses also suggest that the contribution of the leached species to the overall activity is not relevant. In the first run 3.5 mg of Ti was leached to the reaction medium, whereas for the 3rd and successive runs the amount of Ti leached was much smaller (around 0.4–0.6 mg). If the leached homogeneous Ti species would have a significant contribution to the overall activity, the total activity of the latter runs would have been appreciably smaller than that of the first run, and not similar.

The same analyses were carried out with furfural from biomass. As with commercial furfural, Ti is leached in all reaction cycles, especially after the first one. When considering the relative amount of Ti losses in successive runs, we have to take into account that the loading of catalyst for the experiments with biomass-derived furfural was smaller (2 wt%) than that used with commercial furfural (4.6 wt%). In this case, the aggregate loss of Ti represents *ca.* 27% of the total Ti. This slight increase in the leached Ti may be due either to the longer contact time between the furfural and catalyst (when using furfural from biomass, each run takes 24 hours) or to some of the products detected with the furfural from biomass (dihydroxyacetone, acetic acid, and 5-methyl-2-furancarboxaldehyde) that could promote Ti leaching. As for pure furfural, most of the Ti is leached (*ca.* 58%) during the first run. Si leaching also takes place to a slightly higher extent than with “commercial” furfural: Ti leaching represents *ca.* 27% of the initial Ti content, whereas the leached Si accounts for less than 0.4% of the initial Si.

The leaching of Ti is also evidenced by the comparison of the XPS spectra of fresh and used TS-1 catalyst. Fig. 10 compares the Ti 2p core level of both samples, and Table 2 summarises the

main chemical parameters deduced from the XPS analyses. The Ti 2p core level was deconvoluted into two contributions; one is represented by the Ti 2p<sub>3/2</sub> peak at 459.8 ± 0.1 eV, and other is represented by the Ti 2p<sub>1/2</sub> contribution at 458.6 ± 0.2 eV (the corresponding Ti 2p<sub>1/2</sub> levels are at located at 5.7 eV higher BE). The first contribution was assigned to tetrahedral Ti(IV) incorporated in the silicalite framework (Ti<sub>t</sub>), whereas that represented by the peak at 458.6 was assigned to octahedral Ti(IV) in anatase TiO<sub>2</sub> (Ti<sub>o</sub>).<sup>39–41</sup> For very good fitting, a small contribution represented by the Ti 2p<sub>3/2</sub> contribution at *ca.* 457.2 eV was required; this has been assigned to Ti(III) produced by the photoreduction of Ti(IV) within the XPS chamber, driven by the X-ray impact and the ultrahigh vacuum required to record the spectra.<sup>40,41</sup>

The first evidence of leaching arises from the comparison between the XPS Ti/Si ratios of fresh and used samples. The XPS Ti/Si ratio of used samples is 0.027, half the value of the fresh samples (0.052). Moreover, a comparison between the XPS and TXRF Ti/Si ratios of fresh and used samples indicates that the leaching process is very intense at the surface of the TS-1 crystallites. Thus, the XPS value of the fresh sample (0.052) is larger

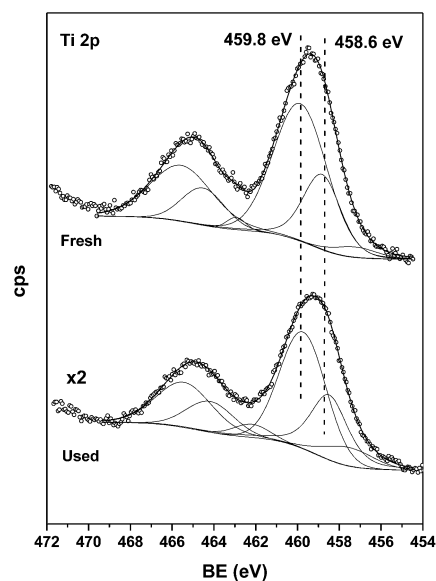


**Fig. 10** Ti 2p core level of fresh and used TS-1 (with commercial furfural).

Table 2 Summary of XPS results in the fresh and used catalysts

	Ti 2p 3/2	Ti/Si	Ti <sub>i</sub> /Si	Ti <sub>o</sub> /Si
Fresh	459.9 (67.4%)	0.052 (0.039) <sup>a</sup>	0.035	0.015
	458.8 (28.5%)			
	457.2 (4.1%)			
Used	459.8 (57.0%)	0.027 (0.032) <sup>a</sup>	0.015	0.008
	458.5 (29.3%)			
	457.2 (13.7%)			

<sup>a</sup> Ti/Si determined from TXRF analysis.

than that determined by TXRF analysis (0.039), perhaps because anatase-like domains are present at the external surface of TS-1. However, the XPS Ti/Si value of the used sample (0.027) is smaller than that determined by TXRF (0.032), indicating the surface is no longer enriched in Ti and therefore that Ti leaching at the surface is very intense. Finally, the Ti leaching process affects both anatase Ti (Ti<sub>o</sub>) and Ti inserted in the silicalite (Ti<sub>i</sub>). Thus, the XPS Ti<sub>o</sub>/Si ratio of the used sample is 0.008, vs. 0.015 for the fresh sample, and the XPS Ti<sub>i</sub>/Si ratio of the used sample is 0.015, vs. 0.035 for the fresh sample.

Taking into account that 20% of Ti was leached upon reutilization, it is quite remarkable that no deactivation was observed when pure furfural is used for the reutilization experiments. A likely hypothesis is that outermost Ti is being leached and innermost active Ti sites remain to conduct the reaction. In this sense, the decrease observed upon reutilization of the surface at Ti/Si by XPS (from 0.052 to 0.027, ca. 50% decrease) is larger than that observed for the bulk TXRF ratio (from 0.039 to 0.032, 18% decrease) indicating that leaching affects mainly to Ti cations located at the surface.

The leaching of Ti also seems to result in slight modifications of the long range order in the framework and in the textural properties of the TS-1: slight but visible modifications of the XRD reflections and of N<sub>2</sub> isotherms are evident when comparing the patterns of the fresh and used samples (see Fig. S10 and SI11 in the ESI† and the discussion therein for further details).

## Conclusions

Titanium silicalite 1 (TS-1) selectively catalyses the aqueous phase oxidation of furfural to maleic acid by using H<sub>2</sub>O<sub>2</sub> as an oxidant agent. A MA yield as high as 78 mol% was obtained under the identified optimum conditions: 4.6 wt% of furfural, 4.6 wt% of catalyst, a H<sub>2</sub>O<sub>2</sub>/furfural mol ratio of 7.5, corresponding to a 12.3 wt% of H<sub>2</sub>O<sub>2</sub> and 24 hours of reaction at 323 K.

All the characterisation data confirm the existence of Ti leaching, which is also associated with a slight leaching of Si. This leaching is very intense during the first run but much less important in successive cycles and affects Ti both in anatase and within the silicalite framework.

Notwithstanding the leaching, when using pure commercial furfural, TS-1 could be reused for six runs without noticeable deactivation. When using furfural directly derived from

biomass, weak but visible deactivation occurs upon reutilisation; this deterioration must be related to the presence of other organic products than furfural.

The amount of H<sub>2</sub>O<sub>2</sub> required when using TS-1 is 2.5 times the value that is stoichiometrically needed. A very selective two-step process has also been demonstrated, which needs a H<sub>2</sub>O<sub>2</sub>/furfural mol ratio of 4.4, an amount of H<sub>2</sub>O<sub>2</sub> much closer to the stoichiometric value (which is 3). This process involves the consecutive utilisation of TS-1 to selectively oxidise furfural to hydroxyfuranone, and consequently, once TS-1 is removed, Amberlyst 70 to catalyse the selective oxidation of hydroxyfuranone to MA.

## Acronym list

FA	Formic acid
FumA	Fumaric acid
Hydroxyfuranone	5-Hydroxy-furan-2(5H)-one
MA	Maleic acid
MAN	Maleic anhydride
SA	Succinic acid

## Acknowledgements

Financial support from Spanish Ministry of Economy and Competitiveness (CTQ2012-38204-C03-01) is gratefully acknowledged.

## Notes and references

- 1 H. H. K. Lohbeck, W. Fuhrmann and N. Fedtke, in *Ullmann's Encyclopedia of Industrial Chemistry*, Weinheim, Germany, 2000, vol. 20, p. 463.
- 2 T. R. Felthouse, J. C. Burnett, B. Horrell, M. J. Mummey and Y.-J. Kuo, Maleic Anhydride, Maleic Acid, and Fumaric Acid, in *Kirk-Othmer Encyclopedia of Chemical Technology Online*, 2001.
- 3 S. Albonetti, F. Cavani and F. Trifirò, *Catal. Rev.: Sci. Eng.*, 1996, **38**, 413.
- 4 D. M. Alonso, S. Wettstein, M. A. Mellmer, E. I. Gurbuz and J. A. Dumesic, *Energy Environ. Sci.*, 2013, **6**, 76.
- 5 A. S. Mamman, J. M. Lee, Y. C. Kim, I. T. Hwang, N. J. Park, Y. K. Hwang, J. S. Chang and J. S. Hwang, *Biofuels, Bioprod. Biorefin.*, 2008, **2**, 438.
- 6 R. Karinen, K. Vilonen and M. Niemela, *ChemSusChem*, **2011**, **4**, 1002.
- 7 E. Mahmoud, D. A. Watson and R. F. Lobo, *Green Chem.*, 2014, **16**, 167.
- 8 E. R. Nielsen, *Ind. Eng. Chem.*, 1949, **41**, 365.
- 9 K. Rajamani, P. Subramanian and M. S. Murthy, *Ind. Eng. Chem. Prod. Res. Dev.*, 1976, **15**, 232.
- 10 M. S. Murthy and K. Rajamani, *Chem. Eng. Sci.*, 1974, **29**, 601.
- 11 D. R. Kreile, V. A. Slavinskaya, M. V. Shimanskaya and E. Y. Lukevits, *Chem. Heterocycl. Compd.*, 1972, **5**, 429.
- 12 N. Alonso-Fagúndez, M. López Granados, R. Mariscal and M. Ojeda, *ChemSusChem*, 1984, **5**, 1984.



- 13 H. Guo and G. Yin, *J. Phys. Chem. C*, 2011, **115**, 17516.
- 14 S. Shi, H. Guo and G. Yin, *Catal. Commun.*, 2011, **12**, 731.
- 15 H. Choudhary, S. Nishimura and K. Ebitani, *Appl. Catal., A*, 2013, **458**, 55.
- 16 H. Choudhary, S. Nishimura and K. Ebitani, *Chem. Lett.*, 2012, **41**, 409.
- 17 L. A. Badovskaya, V. M. Latashko, V. V. Poskonin, E. P. Grunskaya, Z. I. Tyukhteneva, S. G. Rudakova, S. A. Pestunova and A. V. Sarkisyan, *Chem. Heterocycl. Compd.*, 2002, **38**, 1040.
- 18 G. F. Muzychenko, L. A. Badovskaya and V. G. Kul'nevich, *Chem. Heterocycl. Compd.*, 1972, **8**, 1311.
- 19 N. Alonso-Fagúndez, V. Laserna, A. C. Alba-Rubio, M. Mengibar, A. Heras, R. Mariscal and M. López Granados, *Catal. Today*, 2014, **234**, 285.
- 20 A. Cukalovic and C. V. Stevens, *Biofuels, Bioprod. Biorefin.*, 2008, **2**, 505.
- 21 J. Wahlen, B. Moens, D. E. De Vos, P. L. Alsters and P. A. Jacobs, *Adv. Synth. Catal.*, 2004, **346**, 333.
- 22 P. Kumar and R. K. Pandey, *Green Chem.*, 2000, **2**, 29.
- 23 M. G. Clerici, G. Bellussi and U. Romano, *J. Catal.*, 1991, **129**, 159.
- 24 S. B. Kumar, S. P. Mirajkar, G. C. G. Pais, P. Kumar and R. Kumar, *J. Catal.*, 1995, **156**, 163.
- 25 M. A. Uguina, D. P. Serrano, R. Sanz, J. L. G. Fierro, M. López Granados and R. Mariscal, *Catal. Today*, 2000, **61**, 263.
- 26 E. Astorino, J. B. Peri, R. J. Willey and G. Busca, *J. Catal.*, 1995, **157**, 482.
- 27 F. Bonino, A. Damin, G. Ricchiardi, M. Ricci, G. Spanò, R. D'Aloisio, A. Zecchina, C. Lamberti, C. Prestipino and S. Bordiga, *J. Phys. Chem. B*, 2004, **108**, 3573.
- 28 C. D. Wagner, *J. Electron Spectrosc. Relat. Phenom.*, 1983, **32**, 99.
- 29 A. Takagaki, S. Nishimura and K. Ebitani, *Catal. Surv. Asia*, 2012, **16**, 164.
- 30 H. E. Hoydonckx, W. M. Van Rhijn, W. Van Rhijn, D. E. De Vos and P. A. Jacobs, *Furfural and Derivatives*, in *Ullmann's Encyclopedia of Industrial Chemistry*, Wiley-VCH Verlag GmbH & Co. KGaA, 2000.
- 31 K. J. Jung, A. Gaset and J. Molinier, *Biomass*, 1988, **16**, 89.
- 32 W. Zhang, Y. Zhu, S. Niu and Y. Li, *J. Mol. Catal. A: Chem.*, 2011, **335**, 71.
- 33 I. Agirrezabal-Telleria, A. Larreategui, J. Requies, M. B. Güemez and P. L. Arias, *Bioresour. Technol.*, 2011, **102**, 7478.
- 34 I. Agirrezabal-Telleria, I. Gandarias and P. L. Arias, *Bioresour. Technol.*, 2013, **143**, 258.
- 35 C. Li, G. Xiong, J. Liu, P. Ying, Q. Xin and Z. Feng, *J. Phys. Chem. B*, 2001, **105**, 2993.
- 36 L. Wang, G. Xiong, J. Su, P. Li and H. Guo, *J. Phys. Chem. C*, 2012, **116**, 9122.
- 37 G. Ricchiardi, A. Damin, S. Bordiga, C. Lamberti, G. Spanò, F. Rivetti and A. Zecchina, *J. Am. Chem. Soc.*, 2001, **123**, 11409.
- 38 S. Bordiga, A. Damin, F. Bonino, G. Ricchiardi, A. Zecchina, R. Tagliapietra and C. Lamberti, *PCCP Phys. Chem. Chem. Phys.*, 2003, **5**, 4390.
- 39 X. Gao and I. E. Wachs, *Catal. Today*, 1999, **51**, 233.
- 40 G. Moretti, A. M. Salvi, M. R. Guascito and F. Langerame, *Surf. Interface Anal.*, 2004, **36**, 1402.
- 41 F. Langerame, A. M. Salvi, M. Silletti and G. Moretti, *Surf. Interface Anal.*, 2008, **40**, 695.